PHYSICAL REVIEW B VOLUME 56, NUMBER 14 1 OCTOBER 1997-II

First-principles calculations on the atomic and electronic structure of κ-Al_2O_3

Y. Yourdshahyan, C. Ruberto, L. Bengtsson, and B. I. Lundqvist
Department of Applied Physics, Chalmers University of Technology and Göteborg University, S-412 96 Göteborg, Sweden

(Received 28 May 1997)

The atomic and electronic structure and other structural properties of the metastable κ phase of Al_2O_3 have been investigated with a first-principles total-energy method based on density-functional theory at the local-density-approximation level, plane waves, and pseudopotentials. Calculated forces on each atom are used to relax the atomic positions to equilibrium within the restrictions given by what is known about the crystallography of κ-Al_2O_3. Among the structures with stacking-order sequence $AcBcAbCb$, one structure model is found to be the most stable one at zero temperature. Results are presented for atomic configuration, lattice parameters, bulk modulus, band structure, and electronic density of states. There is good agreement with the few available experimental results. [S0163-1829(97)09637-9]

I. INTRODUCTION

Aluminum oxide is a highly insulating material that has a great number of technological applications: as a catalyst support, in electronic-device fabrication, as a cutting-tool material, etc. Alumina, or Al_2O_3, exhibits a number of different phases, such as α, β, γ, η, θ, κ, and χ alumina. The α phase is the stable one, often used as a structural, optical, and electronic material, for instance as a substrate for epitaxial growth of Si in electronic-device fabrication. Both the α and the κ phases of Al_2O_3 are used as wear-resistant coatings on cemented carbides in cutting-tool materials.

Depending on crystallographic definition (crystal or lattice symmetry), α-Al_2O_3 is described as trigonal or rhombohedral.[1–4] Using the lattice symmetry, there is one hexagonal and one rhombohedral crystal system. The crystal structure can be viewed as O atoms arranged in a close-packed hexagonal array (stacking sequence $ABAB$), with the Al atoms occupying two-thirds of the octahedral interstitial sites present between the O layers (space group $R\overline{3}_c$).[2–4]

While many studies have been performed on the α phase, very little is yet known about the κ phase of alumina. A superb way to improve on this situation is to use theoretical modeling. The first step towards an understanding of the physical properties of κ-Al_2O_3 is the determination of its atomic structure.

It is known that the crystal structure of κ-Al_2O_3 belongs to the orthorhombic class containing eight Al_2O_3 molecules per cell (space group $Pna2_1$).[5] The unit cell consists of four O layers in close-packed $ABAC$ stacking sequence and four intervening Al layers. In a recent study[6] we have shown that for the ideal structures it would be energetically prohibitive to have the Al ions in anything but the octahedral positions. This is in agreement with experimental findings,[7] which, however, so far do not definitely point out which of several possible candidates is the real atomic configuration. Our previous calculations[6] have shown that, among the 169 structural models for κ-Al_2O_3 that are consistent with the crystallographic characterization mentioned above, the group of nine configurations with Al atoms in octahedral positions, characterized in Ref. 6 by the stacking-order sequence $AcBcAbCb$, has significantly lower energies.

This type of work is possible thanks to major recent progresses in the accuracy of the density-functional theory (DFT),[8,9,20] and in the methods of solving the Kohn-Sham (KS) equations,[10,11] and in increased computer power.

This paper continues the investigation initiated in our previous work.[6] We allow the ideal structures of the group of nine configurations shown in Ref. 6 to have the lowest total energies to relax. We conclude that among these structures one of the configurations, type II in Table I, is energetically most favorable for the metastable κ-Al_2O_3. The obtained lattice parameters agree well with experimental data.

The organization of the paper is as follows. In Sec. II we account for the calculational method. Section III gives the total-energy values after relaxation of the structural models investigated. The electronic structure of the configuration with the lowest energy is then described quantitatively in terms of the band structure and the density of states. The paper is concluded with a brief discussion in Sec. IV.

II. METHOD OF CALCULATION

In the present work the calculational method is based on DFT,[8,9] plane waves, and pseudopotentials. DFT provides an exact transformation of the many-electron problem onto a set of self-consistent one-electron problems, where the expense is an approximate treatment of the exchange and correlation (XC) energy.[9,12] The XC effects are treated self-consistently within the local-density approximation (LDA).[13,14] Within LDA, the XC potential is a purely local function of the density. Numerous applications have shown the LDA to give results with a useful accuracy for densely packed systems.[15] In addition, we tabulate non-self-consistent generalized-gradient approximation (GGA) results calculated from the self-consistent LDA electronic densities.[16]

The second approximation involves the use of a pseudopotential. It replaces the full ionic potential of the solid with an effective potential for the valence electrons only. This effective potential is often weak, which in a plane-wave representation helps to keep the number of plane waves down. This number is often expressed as an equivalent cutoff energy. The pseudopotentials that we use for oxygen and aluminum are the norm-conserving ones of Troullier and

0163-1829/97/56(14)/8553(6)/$10.00

Martins[17] and Bachelet *et al.*,[18] respectively.

We employ a supercell approach and expand the one-electron wave functions in a plane-wave basis with a cutoff energy of 650 eV, which has previously been found sufficient for the κ-Al_2O_3 crystal.[6] The Kohn-Sham equations are solved iteratively with ever-improving guesses for the self-consistent electronic ground-state density. In each iteration the Kohn-Sham Hamiltonian is diagonalized in the (orthonormalized) subspace of the trial one-electron wave functions and the total-energy gradients with respect to these. The output electronic density is calculated from the orbitals with the lowest energy expectation values and then the input electronic density for the next iteration is constructed by means of a Pulay mixing scheme that tries to guess an accurate input density using information about input and output densities in previous iterations.[10] In order to reduce the number of k points needed, we use a finite electronic temperature of 0.1 eV when determining occupation numbers. All total energies are extrapolated to zero electronic temperature.[19,11] This total-energy pseudopotential implementation has been used previously to successfully describe, e.g., the tiny energy differences of stacking faults in aluminum.[20]

In the self-consistent iterations eight k points in a Monkhorst-Pack[21] sampling are used. This is deemed adequate for the κ-Al_2O_3 crystal.[6]

In order to compare our results for κ-alumina with the α phase and also to test the accuracy of our method we have performed calculations on α-Al_2O_3 using the same technique. We use eight k points and a cutoff energy of 1100 eV and describe the crystal with the rhombohedral unit cell. The parameters describing the crystal are then the lattice parameter a_0 (the edge of the rhombohedron), the rhombohedral angle ϕ, and the internal coordinates w and u specifying the positions of the aluminum and the oxygen atoms, respectively, inside the unit cell.[2–4] To determine the equilibrium structure of α-Al_2O_3 the parameters are first set equal to the experimental ones as given by Lee and Lagerlof.[4] The total energy is then minimized while keeping a_0 and ϕ constant and varying w and u. Thereafter, w and u are kept fixed at their new values and the energy minimized with respect to a_0 and ϕ. The procedure is iterated until no further significant changes could be detected. Our results are $a_0 = 5.091$ Å, $\phi = 55.33°$, $w = 0.3522$, and $u = 0.5562$, in good agreement with other first-principles calculations ($a_0 = 5.123$ Å, $\phi = 55.20°$, $w = 0.3538$, $u = 0.5555$),[22] as well as with the experimental values ($a_0 = 5.1284$ Å, $\phi = 55.28°$, $w = 0.3520$, $u = 0.556$).[4]

III. TOTAL-ENERGY CALCULATION

A. Selection of structure model

Our previous work[6] gives total-energy values for the ideal structure models of the κ phase of Al_2O_3. It thereby succeeds in its aim, namely, to identify nine energetically favored structural models out of the 169 ideal ones that are consistent with the experimentally found crystallographic requirements. In addition, it provides a simple way of distinguishing these nine configurations in terms of the coordination of the Al ions, with only sixfold coordination to O ions in the selected group, while fourfold coordination is present in the energetically disfavored configurations, exclusively or in coexistence with sixfold coordination.[6] In pursuit of the energetically most stable structure of κ-Al_2O_3, we allow in this paper the constituent atoms of the nine ideal configurations to relax.

TABLE I. Calculated total energies for the nine structural configurations of κ-Al_2O_3 with the lowest total energies, after interatomic and volume relaxations. Both LDA and post-LDA GGA values are listed. A, B, and C represent the different O layers, a, b, and c Al layers, and α, β, and γ the vacancy positions of the Al atoms (see, e.g., Ref. 6 for an explanation of the notation used). Note that the Al positions are only octahedral.

Structure			E_{tot} (eV/Al_2O_3)	
Type	No.	Stacking sequence	LDA	GGA
I	1	$Ac^{\alpha}Bc^{\alpha}Ab^{\alpha}Cb^{\alpha}$	−1423.6011	−1430.3432
II	2	$Ac^{\alpha}Bc^{\beta}Ab^{\alpha}Cb^{\gamma}$	−1424.2708	−1430.9829
II	3	$Ac^{\alpha}Bc^{\gamma}Ab^{\alpha}Cb^{\beta}$	−1424.2710	−1430.9834
II	4	$Ac^{\beta}Bc^{\alpha}Ab^{\gamma}Cb^{\alpha}$	−1424.2709	−1430.9830
III	5	$Ac^{\beta}Bc^{\beta}Ab^{\gamma}Cb^{\gamma}$	−1422.5665	−1429.3319
IV	6	$Ac^{\beta}Bc^{\gamma}Ab^{\gamma}Cb^{\beta}$	−1424.0048	−1430.7129
II	7	$Ac^{\gamma}Bc^{\alpha}Ab^{\beta}Cb^{\alpha}$	−1424.2707	−1430.9826
IV	8	$Ac^{\gamma}Bc^{\beta}Ab^{\beta}Cb^{\gamma}$	−1424.0052	−1430.7132
III	9	$Ac^{\gamma}Bc^{\gamma}Ab^{\beta}Cb^{\beta}$	−1422.5669	−1429.3348

For each of the mentioned nine configurations we adopt the following procedure. Initially, the ideal crystal structure is set up. Then the internal atomic coordinates of this theoretically perfect crystal are relaxed, with the constraint that the volume of the cell remain fixed. Second, the total energy as a function of the cell volume is calculated, keeping the relative internal coordinates of the atoms fixed. The total-energy values resulting from these internal and volume relaxations are listed in Table I.

To relax the internal atomic positions we have used the damped molecular-dynamics (MD) method. In each step, the KS equations are first solved to self-consistency, yielding the forces on the atoms in the supercell. Then the MD equations of motion with a damping term are solved according to the calculated forces, giving a displacement of the atomic positions. The residual forces on the atoms after the relaxation are smaller than 0.01 eV/Å.

Due to the symmetry of the unit cell of κ-Al_2O_3, a rotation of 180° around the [010] direction transforms structure Nos. 2, 3, and 5 to 7, 4, and 9, respectively, with numbers as in Table I. As can be seen from Table I, the results from the total-energy calculations support this. Considering the symmetry of the six configurations left, we note that the translation operation $(x + 1/2, y + 1/2, z)$ transforms structure Nos. 2, 4, and 6 to 3, 7, and 8, respectively. This means that there are in fact only four different structure types (labeled I–IV in Table I).

The internal and volume relaxation procedure is iterated for one structure from each of the four types until the ionic positions no longer change significantly. After the relaxation, structure types I and III show a lower symmetry than what has been found experimentally for κ-Al_2O_3. They also show a tendency for volume expansion (see Fig. 1 and Table II), which is not expected at zero temperature. Furthermore, our calculations show that the total energy is higher for these two structure types compared to the other two. We conclude that

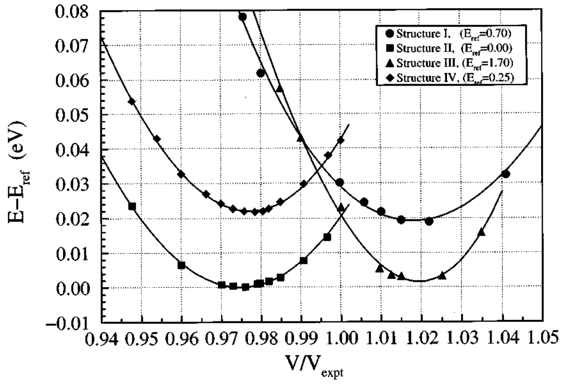

FIG. 1. Calculated total energies of the four different configuration types of κ-Al_2O_3 crystal, listed in Table II, as a function of the crystal volume.

there are only two possible configuration types left in the group for the metastable κ-Al_2O_3, namely types II and IV.

The total energies for these two structures are then calculated as functions of the lattice-constant ratios b/a and c/a, while keeping the crystal volumes and the internal coordinates fixed at their relaxed values. The results for structure type II are shown in Fig. 2.

In order to obtain a reliable accuracy and be able to distinguish between the two remaining structure types, we repeat the whole relaxation procedure until the changes in the total-energy values become smaller than 1 meV/Al_2O_3. The results are shown in Table III. We conclude that both configurations are relatively stable, and, at the same time, that there is a possibility for a κ phase, where the energetic penalty for going from one configuration to another is rather low (0.26 eV/Al_2O_3). Furthermore, we see that the calculations put high demands on the accuracy of the method. Using the results from the total-energy calculations for the optimized structures (Table III) we find structure type II to be the most stable $AcBcAbCb$ structure for κ-Al_2O_3. The atomic coordinates of this selected configuration are given in Table IV, and the crystal structure is shown in Fig. 3(a).

Computer simulations of x-ray powder diffraction (XRD) diffractograms of the different κ-Al_2O_3 structure models, when compared to data from XRD measurements, indicate that all nine structures of Table I are possible.[7] The measured XRD patterns are found most consistent with structure Nos. 2 and 8, though, corresponding to the structure types II and IV, respectively. Reference 7 suggests that structure No. 8 (type IV) should be the right one, but the other structures are never ruled out as possible candidates. In contrast to this, we find that energetically structure type II lies 0.26 eV/Al_2O_3 lower than type IV. We conclude that our findings are not only consistent with this experiment but also show that theoretical calculations can be used to select between different possible structures.

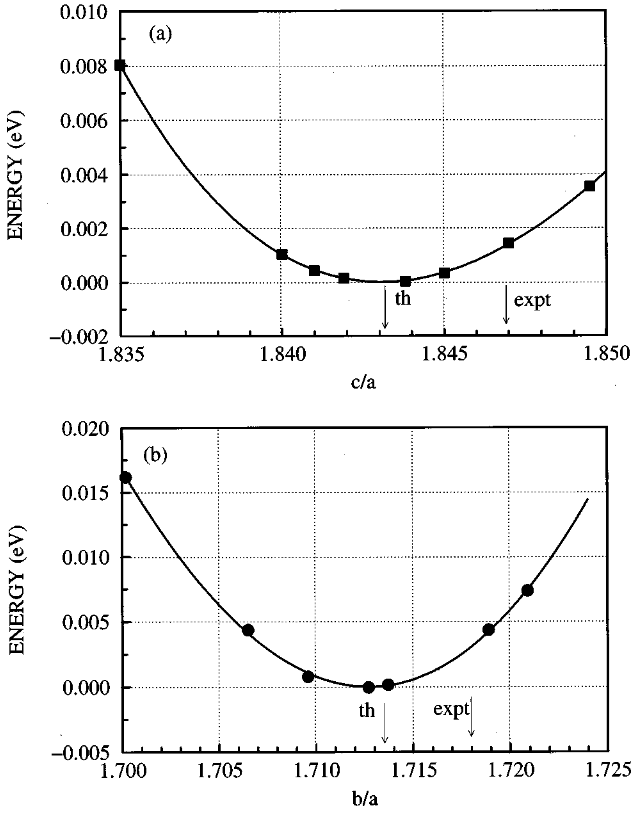

FIG. 2. Calculated total energy for κ-Al_2O_3 crystal type II as a function of b/a and c/a, where a, b, and c are the lattice parameters of the κ-Al_2O_3 unit cell. The arrows marked "expt" denote the experimental values and the other arrows the calculated energy-minima values.

The crystallographic specifications given in Table IV and Fig. 3 show the calculated positions of the atoms in the selected structure. We note that the O planes are relatively intact also after relaxation, while the Al planes are considerably buckled. Upon relaxation, the unit cell contains 12 planes normal to the c axis. Eight of the planes contain two aluminum atoms per unit cell per plane, and four contain six oxygen atoms per unit cell [Fig. 3(a)]. It is interesting to

TABLE II. Calculated total energies after total relaxation for one configuration from each of the four types of κ-Al_2O_3 crystal. ΔE is the energy difference relative to the type with the lowest energy and V/V_{expt} the ratio between the cell volume obtained after relaxation and the one found experimentally.

Structure		E_{tot} (eV/Al_2O_3)		ΔE	
Type	Stacking sequence	LDA	GGA	(eV/Al_2O_3)	V/V_{expt}
I	$Ac^{\alpha}Bc^{\alpha}Ab^{\alpha}Cb^{\alpha}$	-1423.6174	-1430.3602	0.6622	1.019
II	$Ac^{\alpha}Bc^{\beta}Ab^{\alpha}Cb^{\gamma}$	-1424.2758	-1430.9831	0.0000	0.975
III	$Ac^{\beta}Bc^{\beta}Ab^{\gamma}Cb^{\gamma}$	-1422.5710	-1429.3513	1.7086	1.020
IV	$Ac^{\beta}Bc^{\gamma}Ab^{\gamma}Cb^{\beta}$	-1424.0076	-1430.7183	0.2566	0.977

TABLE III. Calculated total energies for the optimized structure types II and IV.

	E_{tot} (eV/Al_2O_3)		ΔE (eV/Al_2O_3)	
Structure	LDA	GGA	LDA	GGA
$Ac^{\alpha}Bc^{\beta}Ab^{\alpha}Cb^{\gamma}$	−1424.2798	−1430.9904	0.0000	0.0000
$Ac^{\beta}Bc^{\gamma}Ab^{\gamma}Cb^{\beta}$	−1424.0230	−1430.7260	0.2568	0.2644

notice that this arrangement is similar to the one for α alumina, where the aluminum atoms lie in two separate planes between consecutive oxygen layers.[23]

In order to compare our theoretical values of the optimized lattice parameters to the experimental ones measured at room temperature, the experimental thermal expansion coefficients[24] have been used to extrapolate between zero and room temperature, assuming that they do not change dramatically in this regime. The results (Table IV) are in excellent agreement with experiments, the differences having the expected sizes considering the fact that in LDA calculations the lattice constants are typically up to 2% smaller than the experimental values.[13]

Other features of the relaxed structural models are noticed upon comparison with the ideal structures. For instance, in the relaxed type-II structure the Al ions have a tendency to form pairwise short-long Al-O bonds of 1.79 and 1.94 Å. The same tendency is noted in the α alumina.[25,26]

By fitting the calculated volume dependence of the energy to the Murnaghan equation of states[27] we obtain a value for the bulk modulus of the type-II κ-Al_2O_3 structure equal to 251.8 GPa. Since, unfortunately, there are no experimental values for the bulk modulus of κ alumina available, we have as a way of comparison used our method to calculate the bulk modulus of the α phase, obtaining a value of 249.1 GPa [the experimental value for α alumina is 252 GPa (Ref. 28)]. These results do not only indicate the high accuracy of the method used, but also that the two phases should not differ significantly in hardness.

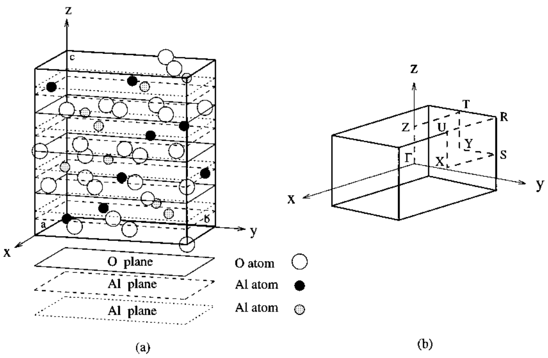

FIG. 3. (a) The calculated crystal structure of κ-Al_2O_3. (b) The Brillouin zone (BZ) of the structure.

B. Band structure and density of states

For our energy-optimized configuration of κ-Al_2O_3 we have calculated the band structure along the symmetry lines in the BZ shown in Fig. 3(b), as presented in Fig. 4. The corresponding orbital-resolved partial densities of states

TABLE IV. Comparison of the crystallographic specification of κ-Al_2O_3 crystal between experimental values (Ref. 24) and our theoretically selected structure.

	Expt. (Room temp.) Measured[a]	Expt. (0 K) Extrapolated	Calculated Structure type II
a (Å)	4.8351	4.831	4.804
V (Å^3)	359.10	357.9	350.16
b/a	1.7189	1.718	1.7137
c/a	1.8482	1.847	1.8435
c/b	1.0753	1.075	1.0757
B (GPa)			251.8
Al-O bonds (Å)			1.79 and 1.94
Al-Al bonds (Å)			2.7
O-O bonds (Å)			2.75
	Calculated atomic positions for crystal structure type II		
Symmetry operations:	$[(x,y,z);\ (1/2-x,1/2+y,1/2+z);\ (1/2+x,1/2-y,z);\ (-x,\ -y,1/2+z)]$		
O atoms:	[(0.958, 0.988, 0.001), (0.054, 0.330, 0.001), (0.010, 0.677, 0.996), (0.674, 0.008, 0.262), (0.653, 0.328, 0.254), (0.661, 0.668, 0.236)]		
Al atoms:	[(0.876, 0.179, 0.098), (0.821, 0.842, 0.153), (0.323, 0.348, 0.394), (0.835, 0.527, 0.355)]		

[a] Reference 24.

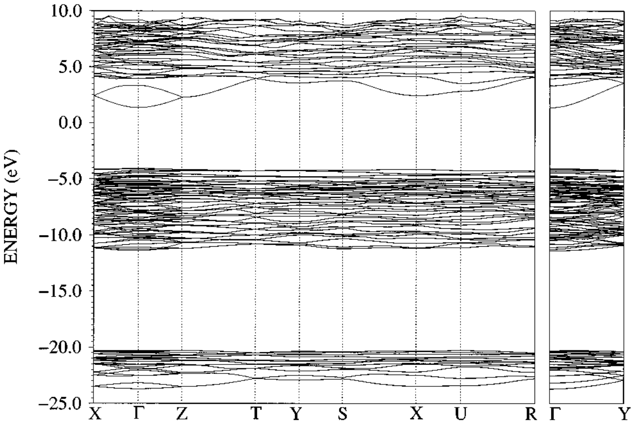

FIG. 4. Calculated band structure of κ-Al_2O_3 structure type II. The symmetry point labeling is shown in Fig. 3(b). The energies are relative to the Fermi level calculated at the electronic temperature of 0.1 eV.

(PDOS) are shown in Fig. 5. The bands are located in three regions: O $2s$ bands between -24 and -20 eV, O $2p$ bands between -12 and -4 eV, and the conduction bands (CB) above 1 eV, mainly due to Al s orbitals. The PDOS show clearly that the bands are dominated by oxygen orbitals: Almost all charge can evidently be associated with the oxygen atoms, implying a highly polar character of the Al-O bonds in κ alumina, as is the case for the α alumina.

The calculated band structure is typical for an insulator material with a large band gap. We obtain a direct band gap of 5.4 eV at the Γ point. Previous results have shown that, when using LDA, the band gap is generally underestimated compared to the experimental one.[25] Once again, there is here a lack of experimental data to compare with. Some comparison can be made to the α phase, for which our calculations give a direct band gap of 6.6 eV at the Γ point, which agrees well with the results 6.31 eV,[26] of previous first-principles calculations on α-Al_2O_3, while the experimental value is 8.8 eV.[29]

From the curvature of the bands we can estimate the electron effective mass of the CB at the Γ point. We obtain the values $0.40m_e$, $0.35m_e$, and $0.40m_e$ along the three directions $\Gamma \rightarrow Z$, $\Gamma \rightarrow X$, and $\Gamma \rightarrow Y$, respectively. The top of the valence band (VB), on the other hand, is very flat, giving very large values for the effective hole masses. The flatness of the VB indicates that the corresponding electrons are tightly bound to the host atoms. The effective electron masses are of the order of those of most semiconductors, indicating that electronic conduction would be possible in κ-Al_2O_3, if somehow the electrons could be excited across the large band gap to the CB.

IV. CONCLUSION

We have performed extensive computations on the κ phase of Al_2O_3, in pursuit of the crystallographic structure of this metastable phase. The calculations are based on the DFT at the LDA level. In Ref. 6 we have shown this ''numerical experiment,'' in principle limited only by the limited validity of the LDA, to give significantly lower energies for a group of nine structural models out of the 169 ideal configurations consistent with what is known about the crystal symmetry. These nine structures are distinguished from the other ones by having Al ions in only octahedral sites in the Al interlayers, i.e., by having Al in only sixfold coordinations. In this paper we have allowed for geometrical relaxation of each of these nine structures and found one structure to have the lowest energy. We have thus taken a further step forward towards the determination of the crystal structure of κ alumina. The results are consistent with the available experimental information, and should help to resolve outstanding uncertainties in the interpretation of the experimental data. However, relaxation of the stacking sequences other than the $AcBcAbCb$ one should also be investigated before drawing definite conclusions about the crystal structure of κ alumina.

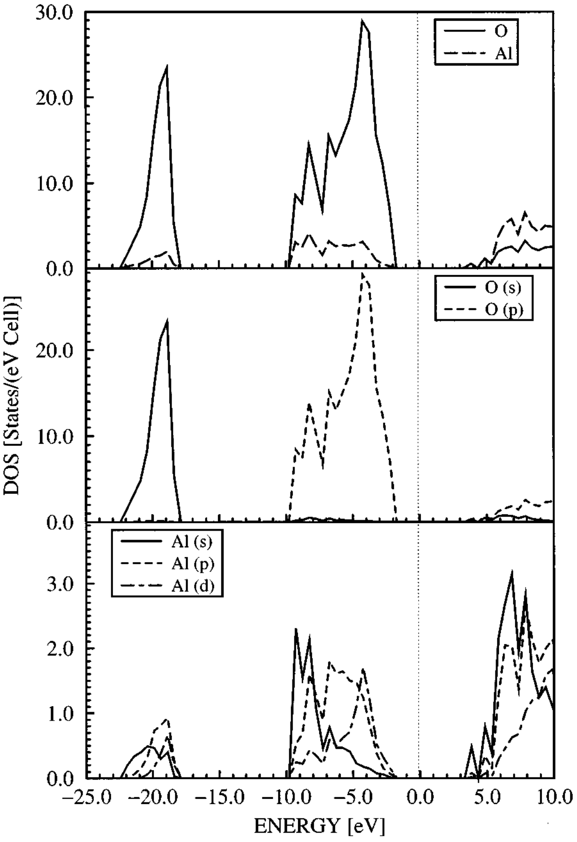

FIG. 5. Calculated orbital-resolved partial DOS of the κ-Al_2O_3 structure type II. The energies are relative to the Fermi level calculated at the electronic temperature of 0.1 eV.

ACKNOWLEDGMENTS

This work originated from discussions with U. Rolander, who has also provided valuable support and help input during the study. The authors acknowledge the essential contributions of U. Engberg for guidance and support. The work was supported by the Swedish National Board for Industrial and Technical Development and the Swedish Research Council for Engineering Sciences.

[1] L. Pauling and S. B. Hendriks, J. Am. Chem. Soc. **47**, 781 (1925).

[2] R. W. G. Wyckoff, *Crystal Structures*, 2nd ed. (Wiley, New York, 1964).

[3] M. L. Kronberg, Acta Metall. **5**, 507 (1957).

[4] W. E. Lee and K. P. D. Lagerlof, J. Electron Microsc. Tech. **2**, 247 (1985).

[5] P. Liu and J. Skogsmo, Acta Crystallogr., Sect. B **47**, 425 (1991).

[6] Y. Yourdshahyan, U. Engberg, L. Bengtsson, B. I. Lundqvist, and B. Hammer, Phys. Rev. B **55**, 8721 (1997).

[7] M. Halvarsson, Ph.D. thesis, Chalmers University of Technology, 1994.

[8] P. Hohenberg and W. Kohn, Phys. Rev. **136**, B864 (1964).

[9] W. Kohn and L. J. Sham, Phys. Rev. **140**, A1133 (1965).

[10] G. Kresse and J. Furthmüller, Comput. Mater. Sci. **6**, 15 (1996).

[11] L. Bengtsson (unpublished).

[12] R. O. Jones and O. Gunnarsson, Rev. Mod. Phys. **61**, 689 (1989).

[13] D. M. Ceperley and B. J. Alder, Phys. Rev. Lett. **45**, 566 (1980).

[14] J. P. Perdew and A. Zunger, Phys. Rev. B **23**, 5048 (1981).

[15] T. Ziegler, Chem. Rev. **91**, 651 (1991).

[16] J. P. Perdew and Y. Wang, Phys. Rev. B **33**, 8800 (1986).

[17] N. Troullier and J. L. Martins, Phys. Rev. B **43**, 1993 (1991).

[18] G. B. Bachelet, D. R. Hamann, and M. Schlüter, Phys. Rev. B **26**, 4199 (1982).

[19] M. J. Gillan, J. Phys.: Condens. Matter **1**, 689 (1989).

[20] B. Hammer, K. W. Jacobsen, V. Milman, and M. C. Payne, J. Phys.: Condens. Matter **4**, 10 453 (1992).

[21] H. J. Monkhorst and J. D. Pack, Phys. Rev. B **13**, 5188 (1976).

[22] I. Manassidis and M. J. Gillan, J. Am. Ceram. Soc. **77**, 335 (1994).

[23] T. J. Godin and J. P. LaFemina, Phys. Rev. B **49**, 7691 (1994).

[24] M. Halvarsson, V. Langer, and S. Vuorinen, Surf. Coat. Technol. **76-77**, 358 (1995).

[25] Yong-Nian Xu and W. Y. Ching, Phys. Rev. B **43**, 4461 (1991).

[26] W. Y. Ching and Yong-Nian Xu, J. Am. Ceram. Soc. **77**, 404 (1994).

[27] F. D. Murnaghan, Proc. Natl. Acad. Sci. USA **30**, 244 (1944).

[28] J. M. Léger, J. Haines, M. Schmidt, J. P. Petitet, A. S. Pereira, and J. A. H. da Jornada, Nature (London) **383**, 401 (1996).

[29] R. H. French, J. Am. Ceram. Soc. **73**, 477 (1990).